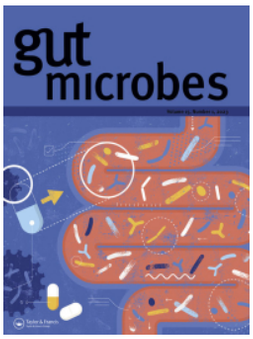

Gut Microbes

ISSN: 1949-0976 (Print) 1949-0984 (Online) Journal homepage: www.tandfonline.com/journals/kgmi20

Muribaculum intestinale negatively impacts glioma growth in mice through the toll-like receptor 2

Francesco Marrocco, Germana Cocozza , Fabrizio Antonangeli , Rizwan Khan , Giuseppe Pietropaolo , Abdechakour Elkihel , Gabriele Favaretto , Xingzi Lin , Romina Mancinelli , Ludovica Maria Busdraghi , Alice Reccagni , Gianluca Scarno , Giuseppe Sciumè , Mattia Laffranchi , Ling Peng , Valerio Iebba , Silvano Sozzani , Giuseppina D'Alessandro & Cristina Limatola

To cite this article: Francesco Marrocco, Germana Cocozza , Fabrizio Antonangeli , Rizwan Khan , Giuseppe Pietropaolo , Abdechakour Elkihel , Gabriele Favaretto , Xingzi Lin , Romina Mancinelli , Ludovica Maria Busdraghi , Alice Reccagni , Gianluca Scarno , Giuseppe Sciumè , Mattia Laffranchi , Ling Peng , Valerio Iebba , Silvano Sozzani , Giuseppina D'Alessandro & Cristina Limatola (2026) ***Muribaculum intestinale*** **negatively impacts glioma growth in mice through the toll-like receptor 2**, Gut Microbes, 18:1, 2623349, DOI: 10.1080/19490976.2026.2623349

To link to this article: https://doi.org/10.1080/19490976.2026.2623349

GUT MICROBES
2026, VOL. 18, NO. 1, 2623349
https://doi.org/10.1080/19490976.2026.2623349

Taylor & Francis
Taylor & Francis Group

RESEARCH ARTICLE

OPEN ACCESS Check for updates

Muribaculum intestinale negatively impacts glioma growth in mice through the toll-like receptor 2

Francesco Marrocco[a], Germana Cocozza[a], Fabrizio Antonangeli[b], Rizwan Khan[a], Giuseppe Pietropaolo[c,d], Abdechakour Elkihel[e], Gabriele Favaretto[b], Xingzi Lin[a], Romina Mancinelli[f], Ludovica Maria Busdraghi[a], Alice Reccagni[a], Gianluca Scarno[c], Giuseppe Sciumè[c], Mattia Laffranchi[c], Ling Peng[e], Valerio Iebba[g], Silvano Sozzani[c,d], Giuseppina D'Alessandro[a,d,1] and Cristina Limatola[d,h,1]

[a]Department of Physiology and Pharmacology, Sapienza University, Rome, Italy; [b]Institute of Molecular Biology and Pathology (IBPM), National Research Council (CNR), Rome, Italy; [c]Department of Molecular Medicine, Sapienza University of Rome, Rome, Italy. Laboratory affiliated to Istituto Pasteur Italia, Rome, Italy; [d]IRCCS Neuromed, Pozzilli, IS, Italy; [e]Aix-Marseille Université, Center Interdisciplinaire de Nanoscience de Marseille, UMR 7325, Equipe Labellisée Ligue Contre le Cancer, CNRS, Marseille, France; [f]Section of Human Anatomy, Department of Anatomic, Histologic, Forensic Medicine and Locomotor Apparatus Sciences, Sapienza University of Roma, Roma, Italy; [g]Gustave Roussy Cancer Campus, ClinicObiome, Villejuif, France; [h]Department of Physiology and Pharmacology, Sapienza University, laboratory affiliated to Istituto Pasteur Italia, Rome, Italy

ABSTRACT

Glioblastoma (GBM) is the most common and malignant brain tumor in adult humans. Recent studies have demonstrated a link between the composition of the gut microbiota and glioma progression. Here, we describe that the growth of glioma in mice is inversely correlated with the relative abundance of the anaerobic bacterium *Muribaculum intestinale* in the feces. We found that *M. intestinale* administration: 1) induced an inflammatory environment in the gut; 2) reduced glioma growth; 3) increased the pro-inflammatory profile of tumor-associated microglial cells and the frequency of CD8+ T cells; and 4) increased the peripheral TNF-*α* levels. The effects induced by *M. intestinale* administration were significantly attenuated upon toll-like receptor 2 (TLR2) silencing using TLR2-targeting siRNA. As a pattern-recognition receptor, TLR2 detects microbial-associated molecular patterns and orchestrates host immune responses to infection. Collectively, these data demonstrate that *M. intestinale* induces a pro-inflammatory response in glioma bearing mice, inhibiting tumor growth via TLR2-dependent signaling.

ARTICLE HISTORY
Received 7 October 2025
Revised 18 December 2025
Accepted 23 January 2026

KEYWORDS
Glioma; gut microbiota; *Muribaculum intestinale*; immune cell activation

Introduction

Among primary brain tumors in adults, glioblastoma (GBM) is the most prevalent and malignant form, characterized by high relapse rate and low survival (14–17 months).[1] Conventional therapies including surgical resection, radiotherapy and chemotherapy fail to effectively prevent recurrence,[2] in part due to the immunosuppressive glioma tumor microenvironment (TME) which limits the efficacy of anti-tumor immune response.[3] In glioma, CD8+ T cells infiltration is maintained at a low level[4] and myeloid cells, including microglia and infiltrating macrophages, adopt an anti-inflammatory pro-tumor phenotype.[5] Therefore, there is an urgent need to explore new possible therapeutic approaches for this fatal disease.

The role of the gut microbiota has been extensively studied in many cancers because of its role in modulating the immune system and the responses to therapies.[6,7] In glioma, gut microbiota modulation through the use of antibiotics, diet or specific nutrient supplementation induces changes in innate and adaptive immune response and affects tumor cell growth.[8-13] Differences have been reported in the gut microbiota and metabolome of healthy individuals and glioma patients, as well as in animal models.[14-16] However, most studies mainly focused on the alterations in the Firmicutes-to-Bacteroidetes ratio.

CONTACT Cristina Limatola cristina.limatola@uniroma1.it IRCCS Neuromed, Pozzilli, IS, Italy; Germana Cocozza germana.cocozza@uniroma1.it Department of Physiology and Pharmacology, Sapienza University, Rome, Italy
[1]These authors sharelast authorship.

Supplemental data for this article can be accessed online at https://doi.org/10.1080/19490976.2026.2623349.

Here, we investigated the composition of microbiota in glioma bearing mice and performed a cross-correlation analysis between tumor volume and the relative abundance of bacterial fecal species. In this experimental model, we revealed a negative association of *Muribaculum intestinale* and a positive association of *Acetatifactor muris* with glioma size. *M. intestinale* is a gram-negative obligate anaerobic bacterium recently discovered in the mouse gut,[14] associated to inflammatory bowel disease.[15-18] *M. intestinale* has pro-inflammatory activity *in vitro*, inducing TNF-α release by the bone marrow-derived dendritic cells through the Toll-like receptor 2 (TLR2).[19] TLR2 is a cell surface pattern receptor which recognizes a wide range of microbial components, including those from gram-negative and gram-positive bacteria.[20] TLRs recognize microbial patterns to control the immune responses against infections and are involved in establishing host-commensal symbiosis.[21] Here, we found that mice treated with *M. intestinale* had reduced tumor volume and developed anti-tumor brain micro-environment characterized by the presence of pro-inflammatory microglial cells and an increased frequency of CD8+ T cells in the GL261 murine model of glioma. These effects were blocked by silencing TLR2 expression in mice, providing evidence for a *M. intestinale*- TLR2-mediated anti-tumor effect.

Materials and methods

Animals and glioma-bearing mice model

This work was conducted in accordance with the ARRIVE guidelines.[22] The approval of all the experiments conducted was granted by the Italian Ministry of Health (authorization no. 775/2020-PR) in accordance with the European Community Council Directive (2010/63/EU) and the Italian d.lgs 26/2014 for the ethical use of animals in laboratory research. Three-week-old male C57BL/6N mice were obtained from Charles River Laboratories (Calco, Italy). Every effort was made to minimize animal suffering and reduce the number of animals used. The necessary sample size was estimated before experiments began. The experiment was restricted to male mice in order to prevent potential sex-dependent influences on the microbial community.[23] Animals were kept in standard cages (two to four per cage) on a 12-h light/dark schedule, receiving sterilized nesting material, autoclaved water, and unrestricted access to autoclaved standard chow.[24] The bedding materials were changed once a week. Murine syngeneic GL261 model was used, as previously reported.[8]

Bacterial cultivation and administration

Bacterial growing culture of *Muribaculum intestinale* (DSM 100739) and *Acetatifactor muris* (DSM 23669) were purchased from Leibniz Institute DSMZ and cultured in Wilkins-Chalgren anaerobe broth under anaerobic condition (hydrogen, 5%; carbon dioxide, 10%; nitrogen 85%) at 37 °C for 4 d. After static growth, bacterial cultures were centrifuged to separate cell pellets and supernatants (4,000 g for 10 min). Oral gavage with 200 µl of fresh anaerobe broth containing 2×10^9 bacteria were performed weekly. To adjust for the effect of oral gavage, a control group underwent oral gavage in fresh Wilkins-Chalgren anaerobe broth.

Orthotopic implantation of murine glioma cells and treatment

Murine GL261 cell line was cultured in DMEM with 100 IU/ml penicillin G, 100 µg/ml streptomycin, 2.5 µg/ml amphotericin B, 2 mM glutamine and 1 mM sodium pyruvate and supplemented with 20% heat-inactivated FBS. Cells were grown at 37 °C in a 5% CO_2-humidified atmosphere and sub-cultivated when 80% confluent. The murine cell line was implanted into the right striatum (−2 mm lateral and +1 mm anteroposterior from the bregma) of mice anesthetized using a stereotaxic apparatus. A total cell suspension of 5×10^4 into 4 µl of sterile PBS was injected with a Hamilton syringe at a rate of 1 µl/min at 3 mm depth. After two days, mice were treated by oral gavage with 2×10^9 bacteria in 0.2 ml of anaerobic broth or the same volume of vehicle (fresh anaerobic broth) once a week for three weeks.

Tumor volume evaluation

After twenty-one days from GL261 injection, mice were sacrificed with transcardiac perfusion of PBS and 4% of PFA, the brains were isolated and quickly frozen. Coronal brain cryosections of 20 µm were prepared for the hematoxylin–eosin staining, as detailed by the manufacturer. Briefly, after staining, brain slices were analyzed by the Image Tool 3.0 software (University of Texas, Health Science Center, San Antonio, TX, USA). Tumor volume was calculated according to the formula (volume = t x ΣA, where t = thickness and A = tumor area/slice).

Colon tissue evaluation

Samples of colon were removed, washed and then fixed in paraformaldehyde (4% v/v) for 12 hours, sucrose 30% and quickly frozen. Coronal colon cryosections of 10 µm were prepared for the hematoxylin–eosin staining, as detailed by the manufacturer. Briefly, after staining, colon samples were evaluated by the percentage of sections with at least an inflammatory cell infiltrate on the total number of sections per group.

Dendrimers preparation and treatment

Calculation of the ratio of siRNA and the amphiphilic dendrimers (ADs)

The ratio of siRNA/dendrimer complexes used depended on the dendrimer-to-RNA charge ratio, defined as the "N/P ratio".[25] The amounts of ADs according to the amount of siRNA in 200 µl for each animal treatment (3 mg/kg) with a 5 N/P ratio.

siRNA delivery and testing efficacy of mRNA silencing

For the intraperitoneal (ip) injection of siRNA or SCRAMBLE delivery using ADs, a stock solution containing the siRNA/AD (or SCRAMBLE/AD) complexes was prepared in a physiologic solution by vortexing before the treatment. Mice were treated via ip two days after tumor cell inoculation every four days for three weeks. The effects of the transfection procedure on mRNA (TLR2) expression were analyzed using quantitative real-time PCR (qRT-PCR) and FACS.

Stool collection and processing, library preparation, sequencing, and bioinformatic analysis

For metagenomic analyzes of microbial composition, fresh stools were collected, frozen, and stored at −80 °C. The fecal bacterial DNA was extracted using a QIAmp Fast DNA Stool Mini Kit (Qiagen) in accordance with the manufacturer's instructions.

For library preparation, the primers Pro341F (CCTACGGGNBGCASCAG) and Pro805R (GACTAC-NVGGGTATCTAATCC) were employed to amplify the V3–V4 region of the 16S rRNA. The resulting libraries were sequenced using Illumina MiSeq technology in 300 bp paired-end mode. Quality control and filtering (sequencing errors, denoising, chimerae detection) of raw fastq files and bioinformatic analyzes were performed as previously reported.[24] Taxonomic analysis was performed using the QIIME 2 *feature-classifier classify-sklearn* plugin with the Greengenes 2 database (gg_2024_09) or NCBI 16 S Microbial Database. Non-biologically relevant bacterial taxa found in blank samples were filtered out, and the residual species were retained for statistical evaluation.

Microbiota statistics

Measurements of α and beta diversities were performed as previously described.[24,26]

The dataset was analyzed through supervised Partial Least Squares Discriminant Analysis (PLS-DA), and the corresponding Variable Importance in Projection (VIP) scores were used to identify bacterial species most relevant for group differentiation. For statistical evaluation, the Mann–Whitney U test was applied to pairwise comparisons, while the Kruskal–Wallis test was used for multiple-group analyzes, adopting a significance threshold of $P \leq 0.05$.

Cell isolation from brain and spleen and flow cytometry

Single cell suspensions were obtained as previously described[8,10] from tumoral hemispheres or spleen as indicated. The mice were perfused intracardially with PBS, after which the brains were rapidly removed and the hemispheres separated and placed into 5 ml of ice-cold HBSS. The tumor-bearing hemispheres were homogenized using a glass-Teflon homogenizer and passed through a 100 µm nylon cell strainer (Becton Dickinson). The spleens were smashed through a 70 µm cell strainer to obtain cells. The spleen was selected to assess systemic TLR2 downmodulation, as it reflects both peripheral and central processes and provides a higher yield of cells than the intestine. Cells were then used for flow cytometric analyzes as follows. Cells were washed and suspended in staining buffer (PBS without Ca^{2+} Mg^{2+}, 1% BSA, 2 mM EDTA, 0.025% NaN_3). Zombie Violet™ Fixable Viability Dye from Bio-Legend was used to exclude dead cells and anti-CD16/32 (clone 2.4G2) was added (10 min) to prevent nonspecific and Fc-mediated binding. The cells were then stained with the indicated antibodies for 20 minutes at 4 °C. The following fluorochrome-conjugated monoclonal antibodies (mAbs) were used, with the clone name indicated in parentheses: CD45 APC-eFluor780 (30-F11), CD11b PE-Cy7 (M1/70), Gr-1 PerCP-Cy5.5 (RB6-8C5), iNOS PE (CXNFT), Arg1 APC (A1exF5) and Ly-6C APC (HK1.4) from eBioscience-Invitrogen (ThermoFisher), as well as CD3e PerCP-Cyanine5.5 (145-2C11) and CD8-FITC (53-6.7). iNOS and Arg1 were stained intracellularly using the BD Cytofix/Cytoperm™ kit according to the manufacturer's instructions. Samples were analyzed using a CytoFLEX cytometer from Beckman Colter. Data were analyzed using FlowJo software v.10.10.0 (BD, FlowJo, Ashland, OR, USA).

Gating strategies to identify microglia, monocytes/macrophages, and CD8 T cells are shown in supplementary Figure 1.

Cell isolation from colon lamina and flow cytometry.

Leukocytes from the large intestine lamina propria were isolated as previously described.[27] Briefly, the intestines were incubated in RPMI 1690 containing Liberase (0.5 mg/mL) and DNase I (0.25 mg/mL), and cells were purified through 40% Percoll gradient.

Flow cytometry analysis was performed on a LSR Fortessa (Becton Dickinson). The antibodies used in this study can be found in supplementary table 1. FlowJo_v10 (Beckton Dickinson), was used for flow cytometry data analysis. Gating strategies to identify leukocytes are shown in supplementary Figure 2.

Total RNA extraction

Mice were sacrificed and transcardially perfused with PBS. The spleen and the distal colon were collected to perform the total RNA extraction. Cells from the spleen were obtained by smashing on a 70 µm cell (Corning) as long as the sample was completely dissected. The suspension was centrifuged (1000g, 10 min, RT) and the pellet lysed in Trizol reagent (Sigma-Aldrich). The distal colon samples (1 cm) were dissected mechanically in Trizol reagent (Sigma-Aldrich) by a cell homogenizer. The total RNA was extracted with Trizol reagent (Sigma-Aldrich) following the manufacturer's protocol. The quality and yield of RNAs were verified using the Nanodrop One System and Qubit (Thermo Scientific).

Bulk RNA sequencing

Isolated total RNA from colon tissue was processed with RNAse-free DNaseI (Invitrogen). Next, total RNA was processed to Nextflex Rapid Directional RNA-Seq kit 2.0 Kit with Nextflex Ribonaut rRNA depletion kit and UDIs (PerkinElmer). The libraries were on Illumina NovaSeq X with 2 × 150 bp paired-end run; Seq throughput: 50 M PE read per sample; Q30 ≥ 85%.

The resulting FASTQ files were pre-processed with Trimmomatic (v0.39)[28] for adapter trimming and low-quality filtering of the reads. Filtered sequence reads were aligned to reference GRCm38 mouse transcriptome with HISAT2 aligner (v2.2.1)[29] and raw counts were obtained with FeatureCounts (subread v2.0.1).[30] GENCODE Gene Set version M27 was used for gene annotation. Transcripts were merged to genes using R (v 4.4.2 (2024-10-31) -- "Pile of Leaves") and biomaRt (v2.62.1).[31] Gene-level normalization

and differential expression analysis were performed with the R package DESeq2 (v1.46.0).[32] We analyzed genes with a total raw count above 10 in at least three samples. R packages EnhancedVolcano (1.24.0) used to generate Volcano plots. DEGs were clustered by functional annotation in gene ontology (GO) analysis using Bioconductor R package clusterProfiler v.4.14.4 with annotation of GO Biological Process categories.[33]

Real time qPCR

To assess TLR2 gene expression, one µg of total spleen RNA was reverse transcribed in a final reaction volume of 20 µl for each sample. Reverse transcription was performed according to the manufacturer's protocol using iScript TM Reverse Transcription Supermix (Biorad) in a thermal cycler (Biorad). Real-time PCR was performed in a CFX Real-Time PCR System (Biorad) using SsoFast TM EvaGreen Supermix (Biorad) according to the manufacturer's instructions. The following primers were used: Glyceraldehyde-3-phosphate dehydrogenase (Gapdh) F 5′-TTCGCAAAACAAGTTCACCA-3′ and R 5′-TCGTTGTGGT TGTAAATGGAA-3′: Tlr2 F 5′-TCTGGGCAGTCT TGA ACATTT- 3′; R 5'-AGAGTCAGGTGATGGA TGTCG-3'.

Statistical analysis

Each figure legend describes both the number of replicates (n) for each experiment and the details of the statistical analyzes.

The data are shown as the mean ± SEM. The precise p-values are specified in the text of the figure legends. The unpaired Student's t-test was utilized to compare two group samples. Where the comparison encompasses more than two groups, a one-way analysis of variance (ANOVA) is employed (Brown–Forsythe and Welch ANOVA tests), with the p-values adjusted for multiplicity. All the statistical analyzes were performed using GraphPad Prism 8 software.

Results

Selective bacterial species correlate with glioma progression in mice

To investigate the effect of glioma transplantation in the brain on the gut microbiome composition, stool samples were collected from mice before (healthy condition, thereafter healthy) and three weeks after tumor cells (glioma condition, thereafter glioma) or PBS injection (sham condition, thereafter sham). A schematic overview of the experimental design and timing of sample collection is shown in Figure 1A. The alpha and beta diversities in the gut microbiome and the composition of the microbial community were determined by 16S rRNA sequencing in the three groups. Figure 1B shows that sample biodiversity, evaluated as inverse Simpson index, was significantly different, while bacterial richness (evaluated as the number of distinct species) did not differ among the three groupsBeta diversity indices were used to describe the ecological diversity between the microbial community samples. As shown in Figure 1C, the beta diversity of the gut microbiome did not significantly differ between the healthy versus sham and glioma cohorts (PERMANOVA $p = 0.2069$, ANOSIM $p = 0.2876$), as previously shown under comparable experimental conditions.[34] However, to possibly identify bacterial species distinctive for the three groups, Partial Least Squares Discriminant Analysis (PLS-DA) model and the VIP score were implemented. Three species were significantly distinctive for the glioma group (*Neglecta timonensis, Harryflintia acetispora and Prevotella stercorea*) and one was enriched in healthy group (*Anaerotignum lactifermentas*), as shown in the pairwise analysis; however, even after this analysis the groups did not clearly clustered (supplementary figure 3).

To investigate potential microbiota-tumor interactions, we performed a cross-correlation analysis between the relative abundance of bacterial species and glioma tumor volumes in glioma-bearing mice ($n = 23$ glioma mice from two independent experiments: 15 mice from previous experiment - Figure 1A–C- and 8 mice from a second experiment, Figure 1D). This analysis allowed us to identify specific bacterial taxa whose presence correlates with tumor progression or suppression. By correlating

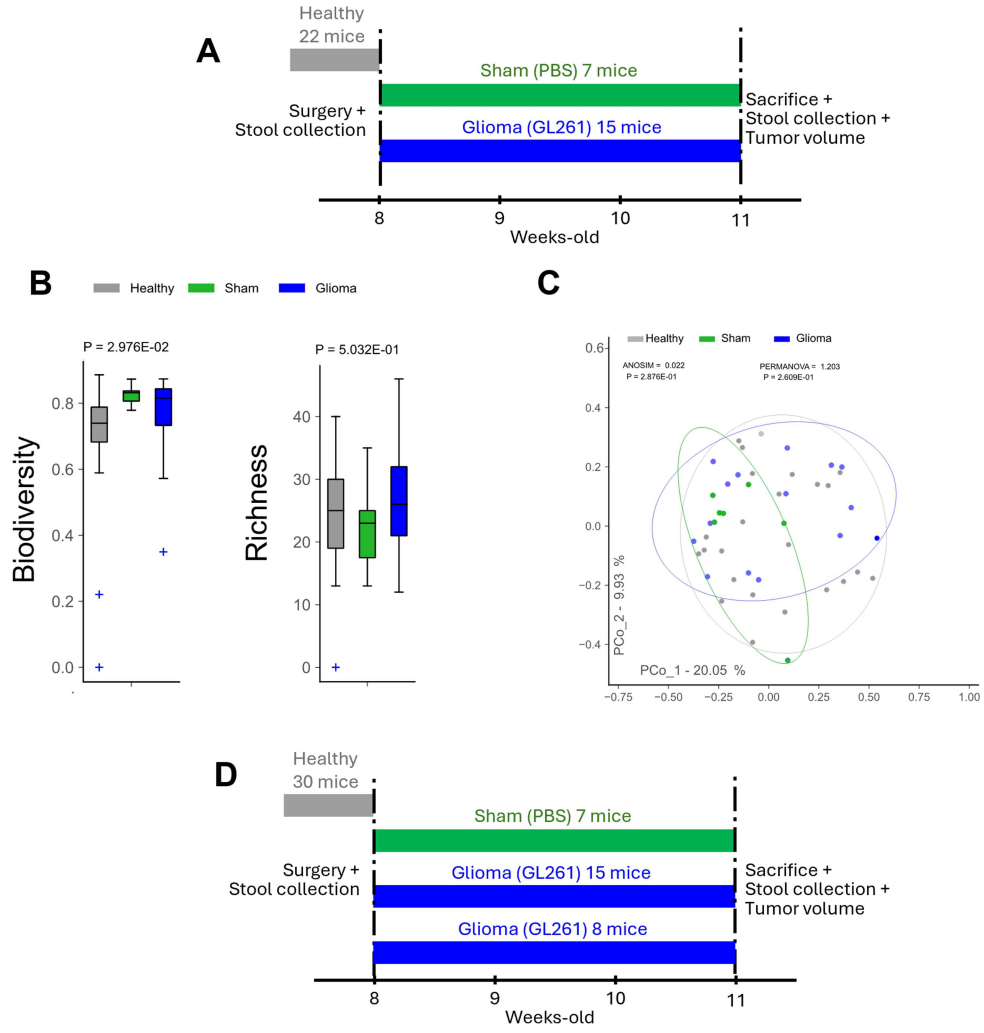

E

	Tumor volume vs. Acetatifcator_muris	Tumor volume vs. Oscillibacter_ruminantium	Tumor volume vs. Pseudoflavonifractor_phocaeensis	Tumor volume vs. Muribaculum_intestinale
Spearman r	0.6192	0.5742	0.6750	-0.6123
95 confidence interval%	0.2659 to 0.8258	0.1999 to 0.8023	0.3528 to 0.8541	-0.8223 to -0.2556
P value	0.0016	0.0042	0.0004	0.0019

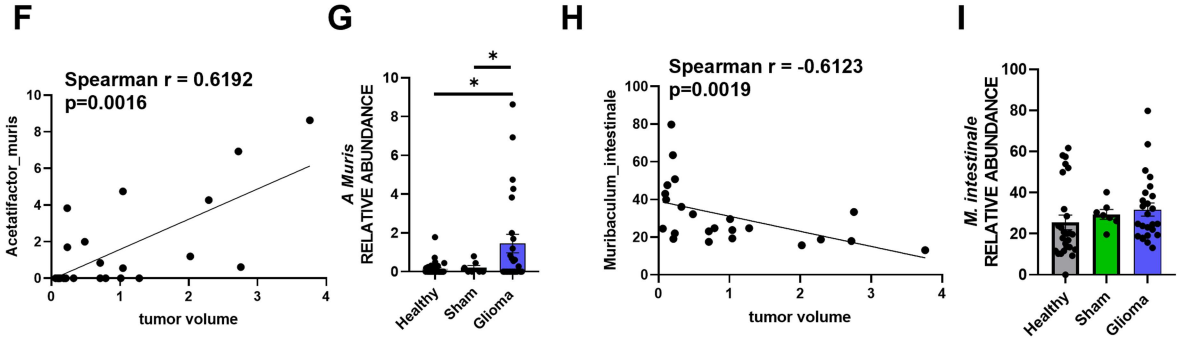

Figure 1. Fecal microbiota in mice with glioma. A. Experimental design. B Alfa-diversity: biodiversity (inverse Simpson) and richness (number of bacterial species) among healthy (Healthy, gray, $n = 22$ biologically independent samples), sham-operated (sham, green, $n = 7$ biologically independent samples) and glioma mice (glioma, blue, $n = 15$ biologically independent samples). C. Beta-diversity following the Bray-Curtis dissimilarity distance algorithm, among healthy, sham

(*Caption on next page*)

and glioma mice. D. Experimental design. E Spearman correlation coefficient analysis between the relative abundance of all bacterial species found in glioma-bearing mice and tumor volumes (23 xy pairs) F. Spearman correlation coefficient graph between tumor volume and *Acetatifactor muris* abundance in glioma mice ($\rho = 0.619$, $p = 0.0016$, $n = 23$ xy pairs). G. Analysis of the relative abundance of fecal *Acetatifactor muris* among healthy (gray, $n = 30$, 0.156 ± 0.057, $^*p = 0.012$ vs glioma), sham-operated (green, $n = 7$, 0.207 ± 0.070, $^*p = 0.017$ vs glioma by Brown-Forsythe ANOVA test) and glioma mice (blue, $n = 23$ 1.450 ± 0.470). H. Spearman correlation coefficient graph between tumor volume and *Muribaculum intestinale* abundance in glioma mice ($\rho = -0.613$, $p = 0.0019$, $n = 23$ xy pairs). I. Analysis of the relative abundance of fecal *Muribaculum intestinale* among healthy (gray, 26.75 ± 3.73, $n = 30$), sham-operated (green, $n = 7$, 29.40 ± 2.38) and glioma (blue, $n = 23$, 31.75 ± 3.17 ns by Brown-Forsythe and Welch ANOVA test).

microbial abundance with tumor size, we aimed to uncover microbial signatures that may influence glioma growth, either by promoting a pro-tumorigenic environment or by supporting anti-tumor immune responses. Results revealed that three bacterial species were positively associated with tumor size, while one species showed a negative correlation, suggesting a potential protective role: in particular, *Acetatifactor muris* is positively associated with tumor volume (Figure 1E) and is also more abundant in glioma mice (Figure 1F), at difference with *Oscillibacter ruminantium* and *Pseudoflavonifractor phocaeensis* (supplementary figure 4). Of note, in sham-operated mice, age-matched with glioma bearing mice, *A. muris* did not increased, thus excluding a time- or surgery-dependent modulatory effect (Figure 1F). As shown in Figure 1E,G, *Muribaculum intestinale* abundance was the only specie negatively associated with tumor volume. Of note, the fecal abundance of *Muribaculum intestinale* did not significantly change in the different experimental groups probably due to the high relative abundance in all groups (Figure 1H).

In summary, in our model, glioma development induced modest changes in gut microbiome diversity, without significantly altering overall community structure. However, specific bacterial species, including *Acetatifactor muris* and *Muribaculum intestinale*, correlate with tumor growth, suggesting potential microbiota–tumor interactions. These findings highlight the relevance of gut microbial composition in glioma progression and warrant further functional studies.

A. muris and M. intestinale administration induces opposite effects on glioma growth in GL261-bearing mice

To determine whether bacterial species associated with tumor progression in glioma-bearing mice influence glioma growth, we treated glioma-bearing mice with either *A. muris* or *M. intestinale*. Fresh anaerobic broth containing 2×10^9 bacteria (*A. muris*, DSM23669; *M. intestinale*, DSM100739) or broth alone (vehicle) was administered via oral gavage to C57BL6 mice brain transplanted with GL261 cells. Treatments began two days after tumor cell implantation and were repeated three times in total (Figure 2A,B). As shown in Figure 2C, mice receiving *A. muris* showed increased tumor volume compared to vehicle-treated mice ($n = 11$ in the vehicle group and $n = 11$ mice in *A.muris* group), whereas mice receiving *M. intestinale* showed a significant decrease in glioma growth (Figure 2C, $n = 9$ mice in the vehicle group and $n = 10$ in *M. intestinal*e group) thus demonstrating that the two species have opposite effects on glioma progression, in accordance with the correlation analyzes shown in Figure 1E,G. However, further studies in additional glioma models are required to generalize these observations.

M. intestinale administration induces an inflammatory environment in the gut of GL261-bearing mice

To better understand the effects induced by *M. intestinale* on glioma bearing mice, we focused our attention on the gut, to explore the hypothesis that the negative effects on tumor growth could be explained by the modulation of gut homeostasis and of its immune component.

We first investigated the presence of *M. intestinale* in terminal stool by NGS analysis of the 16S rRNA gene. As shown in Figure 3A, fecal samples from *M. intestinale*-treated mice described in the previous experimental plan (Figure 2B), showed a mean enrichment of 1.6 times over vehicle-treated mice. To investigate the effects of *M. intestinale* treatment on the gut tissue, bulk mRNA sequencing was performed

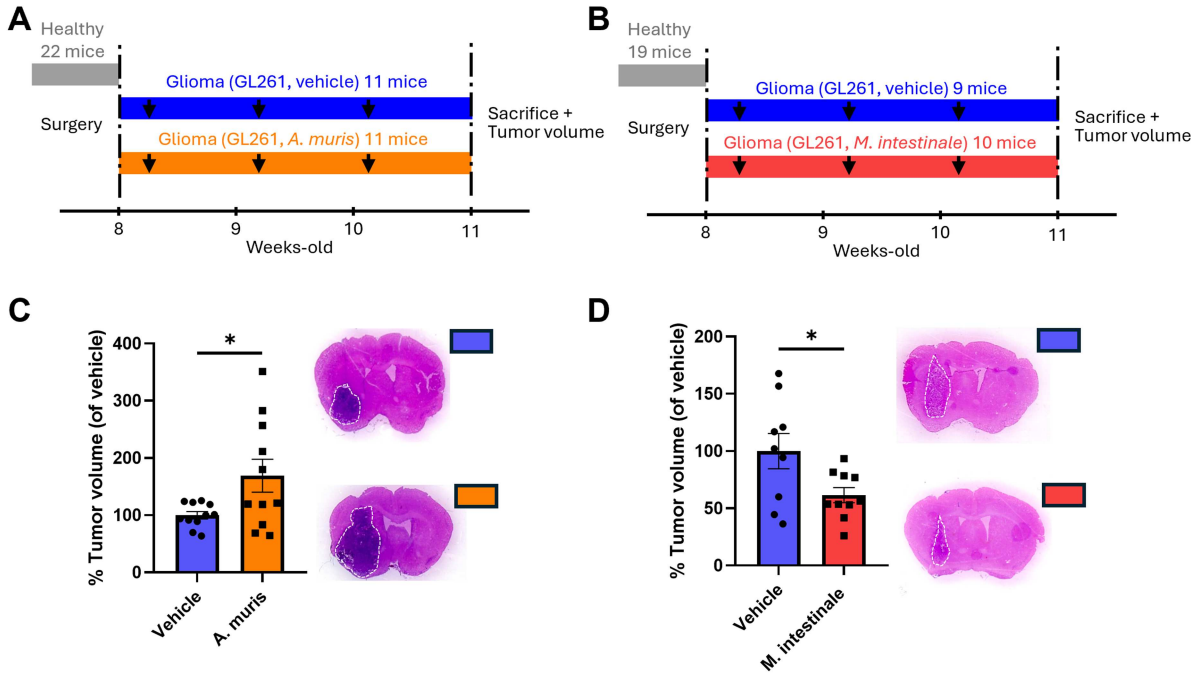

Figure 2. Bacterial administration affects tumor growth. Experimental setup for *A. muris* (A) or *M. intestinale* (B) administration. The black arrows depict the oral gavage of fresh broth (vehicle) or bacterium. C. Tumor volumes in vehicle (blue, $n = 11$, $100.0 \pm 6.4\%$) and *A. muris* treated mice (orange, $n = 11$, $168.9 \pm 28.8\%$, * $p = 0.032$ by unpaired Student's t-test). Right, representative images of brain coronal slices with glioma. D. Tumor volumes in vehicle (blue, $n = 9$, $100.0 \pm 15.4\%$) and *M. intestinale* treated mice (red, $n = 10$, $61.5 \pm 6.5\%$, * $p = 0.014$ by unpaired Student's t-test). Right, representative images of brain coronal slices with glioma stained with Haematoxylin & Eosin.

in the distal colon tissues of vehicle and treated glioma mice. We found that 86 genes were upregulated and 43 were downregulated in *M. intestinale*-treated mice compared to vehicles (Figure 3B). In particular, gene ontology analysis showed that *M. intestinale*-treated mice increase the expression of genes related to gut motor activity while decreasing those related to gut absorption activity (Figure 3C). Note that this variation represents a phenotype typical of an inflamed environment, as reported in patients with inflammatory bowel diseases (IBD).[35] Histological analysis of colon mucosa supported these switch, since mice treated with *M. intestinale* showed higher inflammatory infiltrate in lamina propria and submucosa layer *vs* vehicle treated mice, as reported in Figure 3D. In addition, pooled sera from seven mice per condition revealed that treatment with *M. intestinale* increased the presence of proinflammatory cytokines, including CXCL9, CCL2 and CCL5 (see Supplementary Figure 5), suggesting increased systemic inflammation.

It has been reported that the administration of *M. intestinale* to dendritic cells induces the release of pro-inflammatory cytokines, such as TNFα, through TLR2.[19] We wonder whether this signaling pathway could play a role in the effects of *M. intestinale* on the inflammatory phenotype of the gut in bacteria-treated mice. To evaluate the involvement of TLR2 under our experimental conditions, we co-treated mice with *M. intestinale and scramble siRNA or* TLR2-siRNA delivered by a dendrimer vector,[25,36] as described in Figure 3E, and investigated the effect of treatments on spleen-derived immune cells and on serum TNFα levels. We found that *M. intestinale* treatment increased the expression of Tlr2 as well as the serum levels of TNF-*α* while TLR2 silencing abolished these upregulation (Figure 3F,G) confirming the importance of the receptor signaling in mediating the effects of *M. intestinale*. The efficacy of *in vivo* siRNA treatment was demonstrated by a reduction in the spleen of the number of $TLR2^+$ cells ($23.6 \pm 4.1\%$ less of scramble siRNA), as shown in supplementary Figure 6.

The effect of *M. intestinale* on the gut immunity was investigated by profiling innate lymphocytes and T helper cell subsets in the colonic lamina propria of glioma-bearing mice. We found that mice treatment with *M. intestinale* increased the frequency of innate lymphocytes (namely NK cells, ILC1, ILC2 and

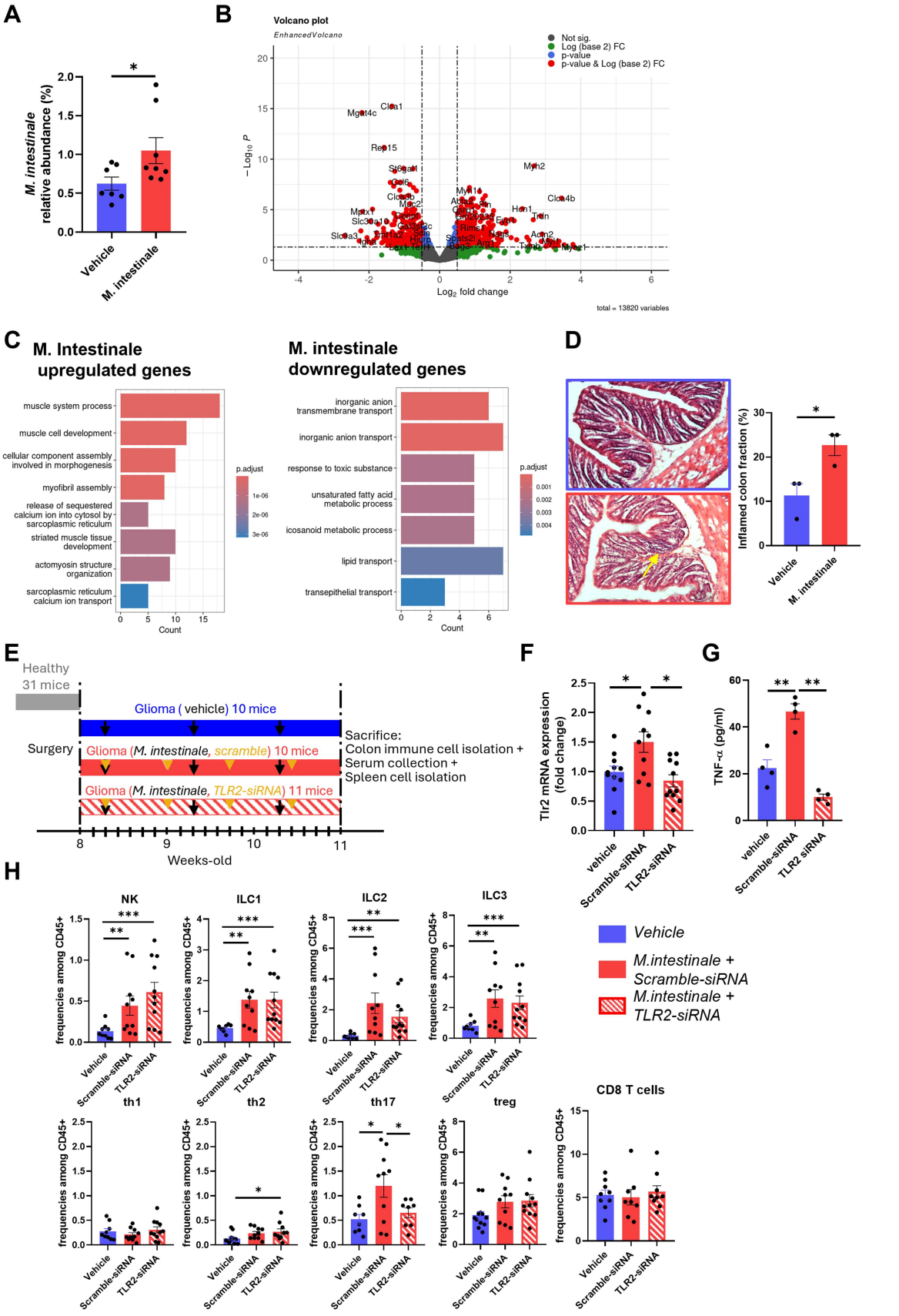

Figure 3. *M. intestinale* administration alters gut environment. A. Analysis of *M. intestinale* enrichment in feces of mice at the end of treatment (blue, vehicle = 0.62 ± 0.08% $n = 7$; red, *M. intestinale* = 1.05 ± 0.16% $n = 8$, * $p = 0.050$ by unpaired Student's t-test). B. Volcano Plot illustrating the differential gene expression in distal colon tissue for *M. intestinale* ($n = 3$

(*Caption on next page*)

independent biological samples) *vs* vehicle-treated glioma mice ($n = 3$ independent biological samples). C. Gene ontology enrichment analysis showing the upregulated and downregulated genes and relative biological processes in distal colon tissues of *M. intestinale* ($n = 3$ independent biological samples) *vs* vehicle-treated glioma mice ($n = 3$ independent biological samples). D. Representative images of H&E-staining of colon tissue showing changes in inflammatory cell infiltrates. Colonic samples from *M.intestinale* mice (upper, blue squared) displayed higher amount of inflammatory infiltrate in lamina propria (yellow arrow) compared to vehicle mice (lower, red squared). Original magnification 10x. Right: quantification of inflamed colon fraction (blue, vehicle $11.3 \pm 2.6\%$, $n = 3$ mice per group/44 total slice; red, *M. intestinale* $22.6 \pm 2.3\%$, $n = 3$ mice/48 total slice, $^{*}p = 0.032$ by unpaired Student's t-test). E. Experimental setup for *M. intestinale* and siRNA loaded dendrimers administration. The black arrows depict the weekly oral gavage of fresh broth (vehicle) or bacterium. Dark yellow triangles depict the intraperitoneal injection (every four days) of scramble-siRNA (scramble) or TLR2-siRNA loaded dendrimers. F. Tlr2 transcript level evaluated as fold increase by real time qPCR over vehicle (blue, 0.99 ± 0.09, $n = 10$), *M.intestinale* + scramble-siRNA (red, 1.48 ± 0.17, $n = 10$, $^{*}p = 0.048$ vs Vehicle) and *M.intestinale* + TLR2-siRNA (red stripes, 0.84 ± 0.10, $n = 11$, $^{*}p = 0.0014$ vs *M.intestinale* + scramble-siRNA by Brown-Forsythe and Welch ANOVA) at the end of experiments. G. Quantification by ELIZA of TNF-α level (pg/ml) in the serum of vehicle (blue, $n = 4$, 22.3 ± 3.6, $^{**}p = 0.0065$ vs siRNA-scramble), *M. intestinale*/scramble siRNA (red, $n = 4$, 46.6 ± 3.2, $^{**}p = 0.0012$ vs siRNA-TLR2 by Brown-Forsythe and Welch ANOVA tests) and *M. intestinale*/siRNA TLR2 (red stripes, $n = 4$, 10.0 ± 1.2) treated mice. H. Quantification of immune cell subset frequencies in colon lamina propria of vehicle (blue, $n = 8$-9), *M. intestinale*/scramble siRNA (red, $n = 10$-11) and *M. intestinale*/siRNA TLR2 (red stripes, $n = 10$-11) treated mice. Statistics by Brown-Forsythe and Welch ANOVA tests.

ILC3) and Th17 cells among the adaptive T cells (Figure 3H). These cells are more abundant in the intestinal mucosa of Chron's Disease (CD) and of IBD patients,[37-41] confirming a gut inflamed environment upon bacterium treatment. In addition, TLR2 silencing specifically reduced the frequency of Th17 cells, consistent with the role of TLR2 in the expansion of this cell population.[42,43]

Taken together, our data show that *M. intestinale* administration triggers several effects in the gut, including an inflammatory gene profile and increased immune cell infiltration, in particular a higher frequency of Th17 cells in the lamina propria and elevated peripheral levels of TNFα, both dependent on TLR2 engagement. However, additional investigations are needed to determine whether additional cell populations contribute to the observed effects.

TLR2 activation mediates the anti-tumor effect of M. intestinale in the brain of GL261-bearing mice

Given the results indicating the induction of a peripheral pro-inflammatory environment in mice upon *M. intestinale* treatment, and considering that a pro-inflammatory tumor microenvironment (TME) can hinder glioma growth,[44,45] we investigated the effects of *M. intestinale* treatment on the TME in glioma-bearing mice. In particular, we wanted to verify the hypothesis that the anti-tumor effect induced by *M. intestinale* administration in mice was mediated by modulation of the TME through the TLR2 pathway. First, we investigated the effect of TLR2 silencing on *M. intestinale*-induced reduction in glioma growth, as described in the scheme of Figure 4A. The data shown in Figure 4B demonstrate that the effect of bacterial treatment on tumor size was absent in TLR2-silenced mice. To exclude the hypothesis that peripheral TLR2 silencing could directly inhibit inflammation and promote tumor progression, we analyzed the effect of TLR2 silencing in untreated glioma bearing mice and we found no differences in tumor growth (supplementary figure 7). We then isolated microglial cells from glioma bearing mice treated with *M. intestinale* to evaluate the expression of representative pro- and anti-inflammatory markers. The results demonstrated an increased protein expression of iNOS and a reduced presence of Arg1. These effects were abolished by TLR2 silencing only for the pro-inflammatory marker iNOS while the anti-inflammatory Arg1 was not affected (Figure 4C). In accordance with the reduction of glioma growth, *M. intestinale*-treated mice showed a reduced presence of tumor infiltrating myeloid cells (among the CD45+ cells) in the brain (Figure 4D) and this reduction was abolished in TLR2 silenced mice. Furthermore, *M. intestinale*-treated mice displayed an increased frequency of CD8+ T cells in the brain (Figure 4E), and higher levels of the degranulation marker CD107 (Figure 4F), suggesting a higher tumor killing activity. TLR2 silencing decreased the CD8+ CD107+ T cells frequency in the brain (Figure 4E), suggesting a receptor mediated mechanism in *M. intestinale*-mediated modulation of TME and glioma growth. However, further studies are necessary to identify additional pattern-recognition receptors responsible of the observed effects.

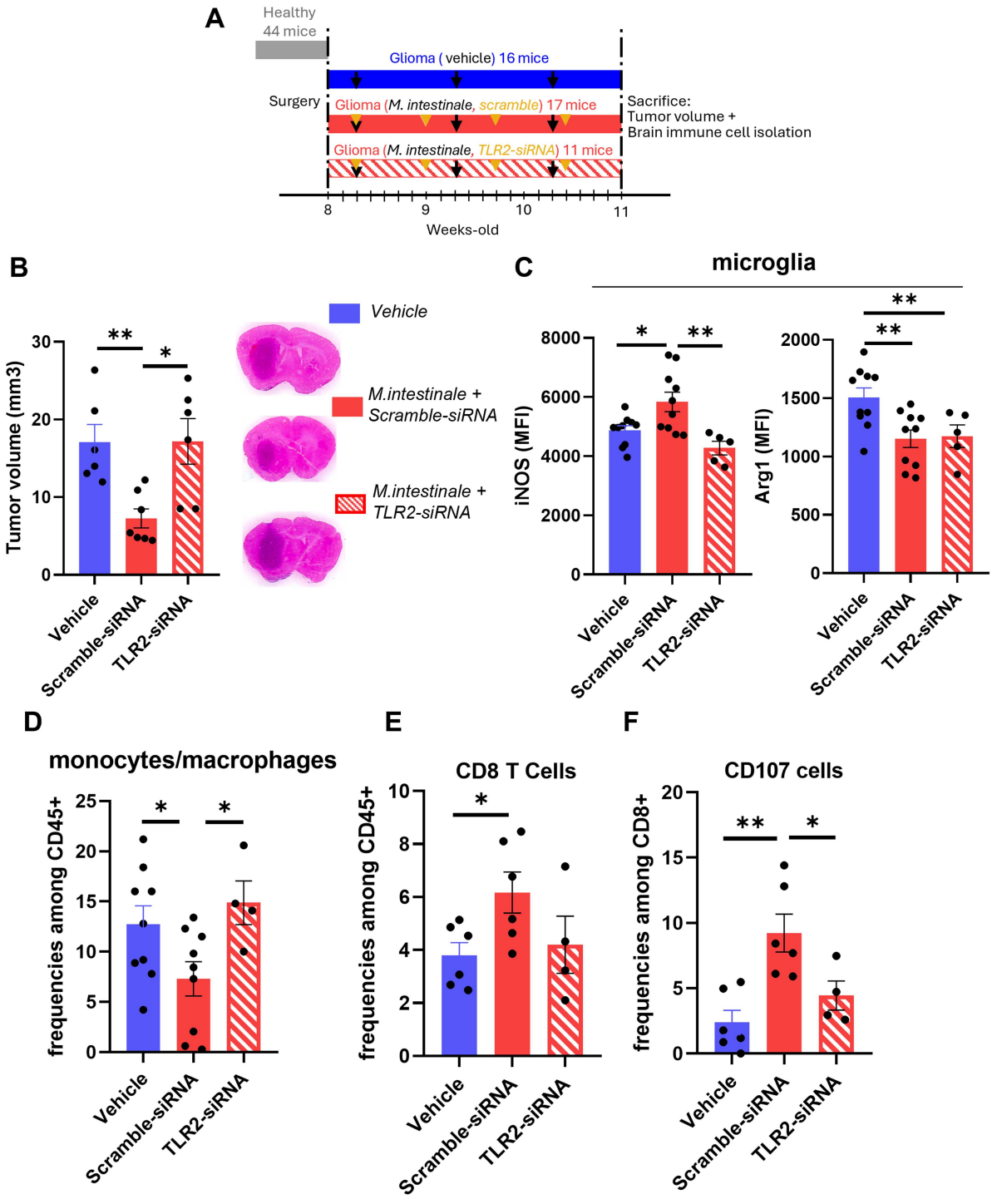

Figure 4. *M. intestinale* affects tumor growth through TLR2. A. Experimental setup for *M. intestinale* and siRNA loaded dendrimers administration. The black arrows depict the weekly oral gavage of fresh broth (vehicle) or bacterium. Dark yellow triangles depict the intraperitoneal injection (every four days) of scramble-siRNA (scramble) or TLR2-siRNA loaded dendrimers. B. Tumor volume evaluation in vehicle (blue, $17.0 \pm 2.2 mm^3$, $n = 6$), *M. intestinale*/scramble-siRNA (red, $7.2 \pm 1.2 mm^3$, $n = 7$, $^{**}p = 0.005$ vs vehicle) and *M. intestinale/* TLR2- siRNA (red stripes, 17.1 ± 2.9 mm^3, $n = 6$, $^{*}p = 0.01$ vs scramble-siRNA) treated mice. Right, Representative images of brain-glioma coronal slices with glioma. C. Protein expression level (MFI, mean fluorescence intensity) as evaluated by flow cytometric analysis of Inos and Arg1 in microglia isolated from vehicle (blue, iNOS = 4869 ± 159, $n = 10$, $^{*}p = 0.020$ vs *M. intestinale*/scramble-siRNA; Arg1 = 1506 ± 82, $n = 10$, $^{**}p = 0.0054$ vs *M. intestinale*/scramble-siRNA), *M. intestinale*/scramble-siRNA (red, Inos = 5834 ± 327, $n = 10$; Arg1 = 1152 ± 75, $n = 10$) and *M. intestinale/* TLR2- siRNA (red stripes, Inos = 4275 ± 228, $n = 5$, $^{**}p = 0.0018$ vs *M. intestinale*/scramble-siRNA; Arg1 = 1174 ± 97, $n = 5$, $^{*}p = 0.027$ vs Vehicle) treated glioma mice. Frequencies of monocytes/macrophages (D) and CD8 positive cells (E) isolated from vehicle (blue, monocytes/

(*Caption on next page*)

macrophages = 12.72 ± 1.86%, $n = 9$, *$p = 0.047$ vs *M. intestinale*/scramble-siRNA; CD8 = 3.79 ± 0.48%, $n = 6$, *$p = 0.030$ vs *M. intestinale*/scramble-siRNA), *M. intestinale*/scramble-siRNA (red, monocytes/macrophages = 7.30 ± 1.70%, $n = 9$; CD8 = 6.16 ± 0.77%, $n = 6$) and *M. intestinale/* TLR2- siRNA (red stripes, monocytes/macrophages = 14.88 ± 2.18%, $n = 4$, *$p = 0.029$ vs vs *M. intestinale*/scramble-siRNA; CD8 = 4.20 ± 1.08%, $n = 4$) treated glioma mice. F. Frequency of CD107 positive cells among CD8 positive cells isolated from vehicle (blue, 2.38 ± 0.93%, $n = 6$, **$p = 0.003$ vs *M. intestinale/* scramble-siRNA), *M. intestinale*/scramble-siRNA (red, 9.22 ± 1.45%, $n = 6$) and *M. intestinale/* TLR2- siRNA (red stripes, 4.43 ± 1.11, $n = 4$, *$p = 0.031$ vs *M. intestinale*/scramble-siRNA) treated glioma mice. Statistics by Brown-Forsythe and Welch ANOVA tests.

Discussion

Here, we investigated the effects of glioma brain transplantation on mouse gut microbiota, to evaluate the hypothesis that glioma could hijack the homeostatic mechanisms of gut-brain communication to increase its chances of colonizing the host brain. We demonstrated that the presence of glioma induces changes in the gut microbiome, and identified bacterial species that are positively or negatively correlated with brain tumor growth. In particular, we find that *Acetatifactor muris*, an anaerobic bacterium isolated from the cecal content of obese mice[46] and recently associated with colonic inflammation in NOD- deficient mice,[47] increased in the fecal samples of glioma mice, and that its administration promotes glioma growth. In contrast, *Muribaculum intestinale,* a bacterial species enriched in the mouse intestine,[14] was not significantly changed in the gut of mice with glioma, while its exogenous administration hampered the growth of brain glioma, favouring the occurrence of an anti-tumor TME, with TLR2-dependent mechanisms.

M. intestinale has been associated with inflammatory bowel disease (IBD) in humans and mice.[15-18] In line with these data, we provide evidence that *M. intestinale* supplementation induced a pro-inflammatory environment in the gut, and gene ontology analysis revealed an increased motility and a reduced absorption capacity in the colonic region, with increased peripheral levels of TNF-α, similar to what reported in gastrointestinal inflammatory diseases.[48] Administration of *M. intestinale* also increased the frequency of infiltrated immune cells in the colonic lamina propria, including the Th17 cells; interestingly, a previous study demonstrated that the administration of *Campylobacter jejuni*, a bacterium associated with irritable bowel syndrome, increased the frequency of CD3+ and CD4+ cells in the colonic lamina and increased TNF-α levels in the serum.[49]

Our finding that *M. intestinale* administration increased serum TNF-α levels through a TLR2-dependent mechanism is in line with previous data showing that this bacterium stimulates inflammatory cytokines through a specific cardiolipin-dependent TLR2 signaling.[19] We expanded these data to demonstrate that other peripheral effects induced in mice upon *M. intestinale*-administration are TLR2-dependent, such as an increased frequency of Th17 cells in the colonic lamina propria. Similarly, in the brain, the effects of *M. intestinale* on the expression of inflammatory cytokines by microglial cells, as well as myeloid and cytotoxic CD3+ T cell infiltration in the glioma-bearing brain hemisphere require TLR2-dependent signals. However, additional pattern-recognition receptors may also contribute to the phenotype observed and future studies employing spatially or cell-resolved transcriptomic approaches will be necessary to pinpoint the precise cellular drivers of the microbiome-glioma interactions in the TME and in the gut.

Bacteria-based therapies for GBM are emerging as innovative strategies to treat this aggressive brain tumor. Studies have shown that bacteria can enhance the anti-tumor immune responses by triggering pyroptosis and promoting the recruitment of immune cells to the tumor region, as demonstrated by engineering *Salmonella typhimurium*[50] and *Porphyromonas gingivalis*.[51] These bacteria penetrate the blood-brain barrier (BBB) and can deliver therapeutic agents directly to the tumor sites, as shown in studies using bacteria loaded with photosensitive nanoparticles.[52] Few studies have explored the natural host antigen-specific responses to selected bacteria in GBM. A recent study demonstrated that administration of *Bifidobacterium lactis* and *Lactobacillus plantarum* reduced tumor growth in glioma-bearing mice through the inhibition of the PI3K/AKT pathway, although the effects on the immune response have not been explored.[34] We report that *M. intestinale* increased the level of TNF-α in the serum of glioma-bearing mice. We speculate that this cytokine could be involved in the anti tumor effects observed in this model, since TNF-α plays a key role in modulating immune responses and triggering anti-tumor activity in

GBM.[45,53-58] Notably, peripheral TNF-α and IL-1α levels below the median have been associated with decreased overall survival in a recent clinical GBM study.[59] In addition, the activation of both innate and adaptive immune responses in glioma mice treated with *M. intestinale* further supports the hypothesis that the gut–brain axis plays a key role in modulating tumor brain growth.

In conclusion, the data reported in this paper, obtained in the GL261 glioma model, add new piece of knowledge to the field of gut-brain communication in glioma and suggest that bacterial administration holds promise as putative adjuvant GBM therapy.

Limitations and future directions

While our study provides compelling evidence that *Muribaculum intestinale* modulates glioma growth in mice, several limitations must be acknowledged. First, all experiments were conducted in male mice. This design choice might overlook known sex-specific differences in microbial composition, immune responses, and glioma biology. Although gliomas occur approximately twice as frequently in males as in females, future work will be necessary to determine whether similar microbiome-tumor interactions occur in female mice. Second, our study only relies on the GL261 syngeneic model. Although widely used, GL261 represents only a limited portion of the genetic, cellular and immunologic heterogeneity characteristic of human GBM. Therefore, the microbiome-tumor interactions observed here may not fully translate to other glioma subtypes or patient-derived systems. Expanding this work to additional, more clinically relevant models, will be critical to strengthen the translatability of our results. Third, we focused on tumor volume at one single experimental endpoint, providing an early proof-of-effect without further investigation of long-term outcomes such as survival, recurrence, or persistence of the immune changes induced by *M. intestinale* administration. These aspects are all worth to be explored in future longitudinal studies designed to capture the durability of the observed responses. Finally, the human gut microbiome is far more diverse and complex than laboratory mice, and M. intestinale is primarily enriched in murine gastrointestinal ecosystem. This raises important questions regarding the translational relevance. While our findings highlight a mechanistic link between gut bacteria and glioma growth in mice, caution is warranted when extrapolating to human GBM. Future work will focusing on human microbiome will be necessary.

Author contributions

CRediT: **Francesco Marrocco:** Formal analysis, Investigation, Writing – original draft; **Germana Cocozza:** Formal analysis, Investigation, Writing – original draft, Writing – review & editing; **Fabrizio Antonangeli:** Formal analysis, Investigation, Writing – original draft; **Rizwan Khan:** Investigation; **Giuseppe Pietropaolo:** Investigation, Writing – original draft; **Abdechakour Elkihel:** Resources, Writing – original draft; **Gabriele Favaretto:** Investigation, Writing – original draft; **Xingzi Lin:** Investigation; **Romina Mancinelli:** Formal analysis, Investigation, Writing – original draft; **Ludovica Maria Busdraghi:** Investigation; **Alice Reccagni:** Investigation; **Gianluca Scarno:** Investigation; **Mattia Laffranchi:** Formal analysis, Investigation, Writing – original draft; **Ling Peng:** Resources, Writing – review & editing; **Valerio Iebba:** Formal analysis, Writing – original draft; **Silvano Sozzani:** Supervision, Writing – original draft; **Cristina Limatola:** Funding acquisition, Project administration, Supervision, Writing – original draft, Writing – review & editing.

Disclosure of potential conflicts of interest

The authors report there are no competing interests to declare.

Funding

This work was supported by Progetto ECS 0000024 Rome Technopole, - CUP B83C22002820006, PNRR Missione 4 Componente 2 Investimento 1.5, finanziato dall'Unione europea – NextGenerationEU to C.L.), by Italian Ministry of Health (PNRR-MAD-2022-12375947, Next Generation EU – PNRR M6C2 - Investimento 2.1 Valorizzazione e potenziamento della ricerca biomedical del SSN to G.P.); Italian Ministry of University and Research (PRIN-2020Z73J5A, PRIN-PNRR-P2022X5ESC to C.L.); by Associazione Italiana per la Ricerca sul Cancro (AIRC2019-IG23010 to C.L.) and (AIRC IG-28719 to G.S.); by Italian Ministry of Health Ricerca Corrente to C.L.; EuroNanoMed project "iNanoGUN" to C.L and L.P. and EU project "HIT-GLIO" (No. 101136835) to L.P.

ORCID

Francesco Marrocco 0000-0002-2732-9119
Giuseppina D'Alessandro 0000-0001-7220-6065

Data availability statement

Raw fastq files were submitted to NCBI Sequence Read Archive (SRA) portal under the Bioproject PRJNA1230168, submission SUB15143986. The RNA-Seq accompanying this paper are available through NCBI's Gene Expression Omnibus (GEO) repository, under accession number GSE290960 located at https://www.ncbi.nlm.nih.gov/geo/query/acc.cgi?acc=GSE290960.

Ethics approval

All the experiments conducted were approved by the Italian Ministry of Health (authorization no.775/2020-PR) under the guidelines of the European Community Council Directive (2010/63/EU) and from Italian D.Lgs 26/2014 for the ethical use of animals in laboratory research.

References

1. Reuss D. Updates on the WHO diagnosis of IDH-mutant glioma. J Neurooncol. 2023;162(3):461–9. doi: 10.1007/s11060-023-04250-5.
2. Molinaro AM, Taylor JW, Wiencke JK, Wrensch MR. Genetic and molecular epidemiology of adult diffuse glioma. Nat Rev Neurol. 2019;15(7):405–17. doi: 10.1038/s41582-019-0220-2.
3. Pearson JRD, Cuzzubbo S, McArthur S, Durrant LG, Adhikaree J, Tinsley CJ, Pockley AG, McArdle SEB. Immune escape in glioblastoma multiforme and the adaptation of immunotherapies for treatment. Front Immunol. 2020;11:582106. doi: 10.3389/fimmu.2020.582106.
4. Wang L, He Z, Fan S, Mo L, Li Y, Yuan X, Xu B, Mou Y, Yin Y. Quantitative analysis of immune cells within the tumor microenvironment of glioblastoma and their relevance for prognosis. Int Immunopharmacol. 2024;142:113109. doi: 10.1016/j.intimp.2024.113109.
5. Poon CC, Sarkar S, Yong VW, Kelly JJP. Glioblastoma-associated microglia and macrophages: targets for therapies to improve prognosis. Brain. 2017;140(6):1548–60. doi: 10.1093/brain/aww355.
6. Matson V, Chervin CS, Gajewski TF. Cancer and the Microbiome—Influence of the commensal microbiota on cancer, immune responses, and immunotherapy. Gastroenterology. 2021;160(2):600–13. doi: 10.1053/j.gastro.2020.11.041.
7. Fernandes MR, Aggarwal P, Costa RGF, Cole AM, Trinchieri G. Targeting the gut microbiota for cancer therapy. Nat Rev Cancer. 2022;22(12):703–22. doi: 10.1038/s41568-022-00513-x.
8. D'Alessandro G, Antonangeli F, Marrocco F, Porzia A, Lauro C, Santoni A, D'Alessandro G, Limatola C. Gut microbiota alterations affect glioma growth and innate immune cells involved in tumor immunosurveillance in mice. Eur J Immunol. 2020;50(5):705–11. doi: 10.1002/eji.201948354.
9. Fan Y, Su Q, Chen J, Wang Y, He S. Gut microbiome alterations affect glioma development and Foxp3 expression in tumor microenvironment in mice. Front Oncol. 2022;12:836953. doi: 10.3389/fonc.2022.836953.
10. Rosito M, Maqbool J, Reccagni A, Giampaoli O, Sciubba F, Antonangeli F, Scavizzi F, Raspa M, Cordella F, Tondo L, et al. Antibiotics treatment promotes vasculogenesis in the brain of glioma-bearing mice. Cell Death Dis. 2024;15(3):210. doi: 10.1038/s41419-024-06578-w.
11. Rosito M, Maqbool J, Reccagni A, Mangano M, D'Andrea T, Rinaldi A, Peruzzi G, Silvestri B, Rosa A, Trettel F, et al. Ketogenic diet induces an inflammatory reactive astrocytes phenotype reducing glioma growth. Cell Mol Life Sci. 2025;82(1):73. doi: 10.1007/s00018-025-05600-4.
12. Silver DJ, Roversi GA, Bithi N, Wang SZ, Troike KM, Neumann CKA, Ahuja GK, Reizes O, Brown JM, Hine C, et al. Severe consequences of a high-lipid diet include hydrogen sulfide dysfunction and enhanced aggression in glioblastoma. J Clin Invest. 2021;131(17):e138276. doi: 10.1172/JCI138276.
13. Kim J, Kim Y, La J, Park WH, Kim HJ, Park SH, Ku KB, Kang BH, Lim J, Kwon MS, et al. Supplementation with a high-glucose drink stimulates anti-tumor immune responses to glioblastoma via gut microbiota modulation. Cell Rep. 2023;42(10):113220. doi: 10.1016/j.celrep.2023.113220.
14. Lagkouvardos I, Pukall R, Abt B, Foesel BU, Meier-Kolthoff JP, Kumar N, Bresciani A, Martínez I, Just S, Ziegler C, et al. The mouse intestinal bacterial collection (miBC) provides host-specific insight into cultured diversity and functional potential of the gut microbiota. Nat Microbiol. 2016;1(10):16131. doi: 10.1038/nmicrobiol.2016.131.
15. Graham DB, Luo C, O'Connell DJ, Lefkovith A, Brown EM, Yassour M, Varma M, Abelin JG, Conway KL, Jasso GJ, et al. Antigen discovery and specification of immunodominance hierarchies for MHCII-restricted epitopes. Nat Med. 2018;24(11):1762–72. doi: 10.1038/s41591-018-0203-7.

16. Pedersen TK, Brown EM, Plichta DR, Johansen J, Twardus SW, Delorey TM, Lau H, Vlamakis H, Moon JJ, Xavier RJ, et al. The CD4+ T cell response to a commensal-derived epitope transitions from a tolerant to an inflammatory state in crohn's disease. Immunity. 2022;55(10):1909–1923. doi: 10.1016/j.immuni.2022.08.016.
17. Dobranowski PA, Tang C, Sauvé JP, Menzies SC, Sly LM. Compositional changes to the ileal microbiome precede the onset of spontaneous ileitis in SHIP deficient mice. Gut Microbes. 2019;10(5):578–98. doi: 10.1080/19490976.2018.1560767.
18. McNamara MP, Singleton JM, Cadney MD, Ruegger PM, Borneman J, Garland T. Early-life effects of juvenile Western diet and exercise on adult gut microbiome composition in mice. J Exp Biol. 2021;224(4):jeb239699. doi: 10.1242/jeb.239699.
19. Bang S, Shin YH, Ma X, Park SM, Graham DB, Xavier RJ, Clardy J. A cardiolipin from *muribaculum intestinale* induces antigen-specific cytokine responses. J Am Chem Soc. 2023;145(43):23422–6. doi: 10.1021/jacs.3c09734.
20. Oliveira-Nascimento L, Massari P, Wetzler LM. The role of TLR2 in infection and immunity. Front Immunol [Internet. 2012;3(79):1–17. doi: 10.3389/fimmu.2012.00079.
21. Round JL, Lee SM, Li J, Tran G, Jabri B, Chatila TA, Mazmanian SK. The toll-like receptor 2 pathway establishes colonization by a commensal of the human microbiota. Science. 2011 May 20;332(6032):974–7. doi: 10.1126/science.1206095.
22. Percie Du Sert N, Hurst V, Ahluwalia A, Alam S, Avey MT, Baker M, Browne WJ, Clark A, Cuthill IC, Dirnagl U, et al. The ARRIVE guidelines 2.0: updated guidelines for reporting animal research. Exp Physiol. 2020;105(9):1459–66. doi: 10.1113/EP088870.
23. Snigdha S, Ha K, Tsai P, Dinan TG, Bartos JD, Shahid M. Probiotics: potential novel therapeutics for microbiota-gut-brain axis dysfunction across gender and lifespan. Pharmacol Ther. 2022;231:107978. doi: 10.1016/j.pharmthera.2021.107978.
24. Marrocco F, Khan R, Reccagni A, Lin X, Delli Carpini M, Iebba V, D'Alessandro G, Limatola C. Fecal or bacterial transplantation in mice transfer environment-induced brain plasticity and associated behavioral changes. Front Physiol. 2025;16:1572854. doi: 10.3389/fphys.2025.1572854.
25. Chen J, Ellert-Miklaszewska A, Garofalo S, Dey AK, Tang J, Jiang Y, Clément F, Marche PN, Liu X, Kaminska B, et al. Synthesis and use of an amphiphilic dendrimer for siRNA delivery into primary immune cells. Nat Protoc. 2021;16(1):327–51. doi: 10.1038/s41596-020-00418-9.
26. Marrocco F, Delli Carpini M, Garofalo S, Giampaoli O, De Felice E, Di Castro MA, Maggi L, Scavizzi F, Raspa M, Marini F, et al. Short-chain fatty acids promote the effect of environmental signals on the gut microbiome and metabolome in mice. Commun Biol. 2022;5(1):517. doi: 10.1038/s42003-022-03468-9.
27. Scarno G, Mazej J, Laffranchi M, Di Censo C, Mattiola I, Candelotti AM, Pietropaolo G, Stabile H, Fionda C, Peruzzi G, et al. Divergent roles for STAT4 in shaping differentiation of cytotoxic ILC1 and NK cells during gut inflammation. Proc Natl Acad Sci U S A. 2023;120(40):e2306761120. doi: 10.1073/pnas.2306761120.
28. Bolger AM, Lohse M, Usadel B. Trimmomatic: a flexible trimmer for illumina sequence data. Bioinformatics. 2014;30(15):2114–20. doi: 10.1093/bioinformatics/btu170.
29. Kim D, Paggi JM, Park C, Bennett C, Salzberg SL. Graph-based genome alignment and genotyping with HISAT2 and HISAT-genotype. Nat Biotechnol. 2019;37(8):907–15. doi: 10.1038/s41587-019-0201-4.
30. Liao Y, Smyth GK, Shi W. The subread aligner: fast, accurate and scalable read mapping by seed-and-vote. Nucleic Acids Res. 2013;41(10):e108. doi: 10.1093/nar/gkt214.
31. Durinck S, Spellman PT, Birney E, Huber W. Mapping identifiers for the integration of genomic datasets with the R/Bioconductor package biomaRt. Nat Protoc. 2009;4(8):1184–91. doi: 10.1038/nprot.2009.97.
32. Love MI, Huber W, Anders S. Moderated estimation of fold change and dispersion for RNA-seq data with DESeq2. Genome Biol. 2014;15(12):550. doi: 10.1186/s13059-014-0550-8.
33. Yu G, Wang LG, Han Y, He QY. clusterProfiler: an R package for comparing biological themes among gene clusters. OMICS J Integr Biol. 2012;16(5):284–7. doi: 10.1089/omi.2011.0118.
34. Wang L, Li S, Fan H, Han M, Xie J, Du J, Peng F. Bifidobacterium lactis combined with lactobacillus plantarum inhibit glioma growth in mice through modulating PI3K/AKT pathway and gut microbiota. Front Microbiol. 2022;13:986837. doi: 10.3389/fmicb.2022.986837.
35. Barros LL, Farias AQ, Rezaie A. Gastrointestinal motility and absorptive disorders in patients with inflammatory bowel diseases: prevalence, diagnosis and treatment. World J Gastroenterol. 2019;25(31):4414–26. doi: 10.3748/wjg.v25.i31.4414.
36. Garofalo S, Cocozza G, Porzia A, Inghilleri M, Raspa M, Scavizzi F, Aronica E, Bernardini G, Peng L, Ransohoff RM, et al. Natural killer cells modulate motor neuron-immune cell cross talk in models of amyotrophic lateral sclerosis. Nat Commun. 2020;11(1):1773. doi: 10.1038/s41467-020-15644-8.
37. Takayama T, Kamada N, Chinen H, Okamoto S, Kitazume MT, Chang J, Matuzaki Y, Suzuki S, Sugita A, Koganei K, et al. Imbalance of NKp44+NKp46– and NKp44–NKp46+ natural killer cells in the intestinal mucosa of patients with crohn's disease. Gastroenterology. 2010;139(3):882–892. doi: 10.1053/j.gastro.2010.05.040.
38. Bernink JH, Peters CP, Munneke M, Te Velde AA, Meijer SL, Weijer K, Hreggvidsdottir HS, Heinsbroek SE, Legrand N, Buskens CJ, et al. Human type 1 innate lymphoid cells accumulate in inflamed mucosal tissues. Nat Immunol. 2013;14(3):221–9. doi: 10.1038/ni.2534.

39. Langer V, Vivi E, Regensburger D, Winkler TH, Waldner MJ, Rath T, Schmid B, Skottke L, Lee S, Jeon NL, et al. IFN-γ drives inflammatory bowel disease pathogenesis through VE-cadherin–directed vascular barrier disruption. J Clin Invest. 2019;129(11):4691–707. doi: 10.1172/JCI124884.
40. Forkel M, Van Tol S, Höög C, Michaëlsson J, Almer S, Mjösberg J. Distinct alterations in the composition of mucosal innate lymphoid cells in newly diagnosed and established crohn's disease and ulcerative colitis. J Crohns Colitis. 2019;13(1):67–78. doi: 10.1093/ecco-jcc/jjy119.
41. Zhao J, Lu Q, Liu Y, Shi Z, Hu L, Zeng Z, Tu X, Xiao Z, Xu Q. Th17 Cells in Inflammatory Bowel Disease: Cytokines, Plasticity, and Therapies. J Immunol Res. 2021;2021:1–14.
42. Nyirenda MH, Sanvito L, Darlington PJ, O'Brien K, Zhang GX, Constantinescu CS, Bar-Or A, Gran B. TLR2 stimulation drives human naive and effector regulatory T cells into a Th17-Like phenotype with reduced suppressive function. J Immunol. 2011;187(5):2278–90. doi: 10.4049/jimmunol.1003715.
43. Marks KE, Flaherty S, Patterson KM, Stratton M, Martinez GJ, Reynolds JM. Toll-like receptor 2 induces pathogenicity in Th17 cells and reveals a role for IPCEF in regulating Th17 cell migration. Cell Rep. 2021;35(13):109303. doi: 10.1016/j.celrep.2021.109303.
44. Grimaldi A, D'Alessandro G, Golia MT, Grössinger EM, Di Angelantonio S, Ragozzino D, D'Alessandro G, Santoro A, Esposito V, Wulff H, et al. KCa3.1 inhibition switches the phenotype of glioma-infiltrating microglia/macrophages. Cell Death Dis. 2016;7(4):e2174. doi: 10.1038/cddis.2016.73.
45. Malone K, Dugas M, Earl N, Alain T, LaCasse EC, Beug ST. Astrocytes and the tumor microenvironment inflammatory state dictate the killing of glioblastoma cells by smac mimetic compounds. Cell Death Dis. 2024;15(8):592. doi: 10.1038/s41419-024-06971-5.
46. Pfeiffer N, Desmarchelier C, Blaut M, Daniel H, Haller D, Clavel T. Acetatifactor muris gen. Nov., sp. Nov., a novel bacterium isolated from the intestine of an obese mouse. Arch Microbiol. 2012;194(11):901–7. doi: 10.1007/s00203-012-0822-1.
47. Lee C, Hong SN, Paik NY, Kim TJ, Kim ER, Chang DK, Kim YH. CD1d modulates colonic inflammation in NOD2−/− mice by altering the intestinal microbial composition comprising acetatifactor muris. J Crohns Colitis. 2019;13(8):1081–91. doi: 10.1093/ecco-jcc/jjz025.
48. Akiho H. Cytokine-induced alterations of gastrointestinal motility in gastrointestinal disorders. World J Gastrointest Pathophysiol. 2011;2(5):72. doi: 10.4291/wjgp.v2.i5.72.
49. Bereswill S, Ekmekciu I, Escher U, Fiebiger U, Stingl K, Heimesaat MM. Lactobacillus johnsonii ameliorates intestinal, extra-intestinal and systemic pro-inflammatory immune responses following murine campylobacter jejuni infection. Sci Rep. 2017;7(1):2138. doi: 10.1038/s41598-017-02436-2.
50. Zhang Y, Xi K, Fu Z, Zhang Y, Cheng B, Feng F, Dong Y, Fang Z, Shen J, Wang M, et al. Stimulation of tumoricidal immunity via bacteriotherapy inhibits glioblastoma relapse. Nat Commun. 2024;15(1):4241. doi: 10.1038/s41467-024-48606-5.
51. Chen Q, Zheng Y, Chen X, Xing Y, Zhang J, Yan X, Wu D. Bacteria synergized with PD-1 blockade enhance positive feedback loop of cancer Cells-M1 Macrophages-T cells in glioma. Adv Sci. 2024;11(20):2308124. doi: 10.1002/advs.202308124.
52. Sun R, Liu M, Lu J, Chu B, Yang Y, Song B, Wang H, He Y. Bacteria loaded with glucose polymer and photosensitive ICG silicon-nanoparticles for glioblastoma photothermal immunotherapy. Nat Commun. 2022;13(1):5127. doi: 10.1038/s41467-022-32837-5.
53. Look T, Puca E, Bühler M, Kirschenbaum D, De Luca R, Stucchi R, Ravazza D, Di Nitto C, Roth P, Katzenelenbogen Y, et al. Targeted delivery of tumor necrosis factor in combination with CCNU induces a T cell–dependent regression of glioblastoma. Sci Transl Med. 2023;15(697):eadf2281. doi: 10.1126/scitranslmed.adf2281.
54. Schiller JH, Storer BE, Witt PL, Alberti D, Tombes MB, Arzoomanian R, Proctor RA, McCarthy D, Brown RR, Voss SD, et al. Biological and clinical effects of intravenous tumor necrosis factor-alpha administered three times weekly. Cancer Res. 1991;51(6):1651–8.
55. Asher A, Mulé JJ, Reichert CM, Shiloni E, Rosenberg SA. Studies on the anti-tumor efficacy of systemically administered recombinant tumor necrosis factor against several murine tumors in vivo. J Immunol Baltim Md 1950. 1987;138(3):963–74. doi: 10.4049/jimmunol.138.3.963.
56. Enderlin M, Kleinmann EV, Struyf S, Buracchi C, Vecchi A, Kinscherf R, Kiessling F, Paschek S, Sozzani S, Rommelaere J, et al. TNF-α and the IFN-γ-inducible protein 10 (IP-10/CXCL-10) delivered by parvoviral vectors act in synergy to induce antitumor effects in mouse glioblastoma. Cancer Gene Ther. 2009;16(2):149–60. doi: 10.1038/cgt.2008.62.
57. Beug ST, Cheung HH, Sanda T, St-Jean M, Beauregard CE, Mamady H, Baird SD, LaCasse EC, Korneluk RG. The transcription factor SP3 drives TNF-α expression in response to smac mimetics. Sci Signal. 2019;12(566), eaat9563. doi: 10.1126/scisignal.aat9563.
58. Beug ST, Beauregard CE, Healy C, Sanda T, St-Jean M, Chabot J, Walker DE, Mohan A, Earl N, Lun X, et al. Smac mimetics synergize with immune checkpoint inhibitors to promote tumour immunity against glioblastoma. Nat Commun. 2017;8(1), 14278. doi: 10.1038/ncomms14278.
59. Cavalheiro VJ, Campos ACP, Lima LGCA, Roça CT, Docema MFL, Lancellotti CLP, Martinez RC, Pagano RL, Chammas R, Teixeira MJ, et al. Unraveling the peripheral and local role of inflammatory cytokines in glioblastoma survival. Cytokine. 2023;161:156059. doi: 10.1016/j.cyto.2022.156059.